ever, continuous culture models have been applied outside the laboratory [A. F. Gaudy and E. T. Gaudy, *Annu. Rev. Microbiol.* **20**, 319 (1966)].
15. The nitrate concentrations were followed along isohalines from Anadyr Strait to the most northerly section sampled in (*4*), and the average change taken as ΔNO_3^-.
16. A carbon productivity of 2.05 g/m^2 per day was recorded recently at the plume edge (*9*), and 4.1 g/m^2 per day was measured in the plume center (*6*).
17. M. J. Dagg *et al.*, *Deep-Sea Res.* 29 (1A), 45 (1982).
18. S. Stoker, in *The Eastern Bering Sea Shelf: Oceanography and Resources*. D. W. Hood and J. A. Calder, Eds. (Univ. of Washington Press, Seattle, 1981), pp. 1069–1090.
19. J. J. Walsh, *Prog. Oceanogr.* **12**, 1 (1983).
20. R. W. Eppley and B. J. Peterson, *Nature (London)* **282**, 677 (1979).
21. D. W. Hood, in *The Eastern Bering Sea Shelf: Oceanography and Resources*, D. W. Hood and J. A. Calder, Eds. (Univ. of Washington Press, Seattle, 1981), pp. 347–358.
22. J. J. Walsh, G. T. Rowe, R. L. Iverson, C. P. McRoy, *Nature (London)* **291**, 196 (1981).
23. J. L. Sarmiento and J. R. Toggweiler, *ibid.* **308**, 621 (1984).
24. E. B. Cohen, M. D. Grosslein, M. P. Sissenwine, F. Steimle, W. R. Wright, *Can. Spec. Publ. Fish. Aquat. Sci.* **59**, 95 (1982).
25. M. J. Dagg and J. T. Turner, *Can. J. Fish. Aquat. Sci.* **39**, 979 (1982).
26. J. J. Walsh, *Nature (London)* **290**, 300 (1981).
27. We thank L. Coachman and two anonymous reviewers for helpful comments. Supported by NSF grants DPP-8300916 and DPP-7623340. Contribution 552, Institute of Marine Science, University of Alaska, Fairbanks.

2 April 1984; accepted 16 May 1984

Side-Scan Sonar Assessment of Gray Whale Feeding in the Bering Sea

Abstract. *Side-scan sonar was used to map and measure feeding pits of the California gray whale over 22,000 square kilometers of the northeastern Bering Sea floor. The distribution of pits, feeding whales, ampeliscid amphipods (whale prey), and a fine-sand substrate bearing the amphipods were all closely correlated. The central Chirikov Basin and nearshore areas of Saint Lawrence Island supply at least 6.5 percent of the total gray whale food resource in summer. While feeding, the whales resuspend at least 1.2 × 10^8 cubic meters of sediment annually; this significantly affects the geology and biology of the region.*

The migratory habits of California gray whales (*Eschrichtius robustus*) allow them to be accurately censused (*1*), and their benthic mode of feeding leaves a measurable record of the amount of prey consumed. These factors provide an opportunity to quantify the feeding ecology of gray whales. Primarily coastal-dwelling, the whales calve and breed in lagoons in Baja California in winter and migrate to feeding grounds in the Bering and Chukchi seas in summer. They feed principally on infaunal amphipods (*2*). Although they do feed during migration (*2*), most of their nourishment comes from foraging in the 1 × 10^6 km^2 of Arctic shelf that constitutes their northern feeding grounds (*3*, *4*).

Mud plumes in the water column near gray whales are indications of benthic feeding activity (*5*). Such behavior has been observed in a captive gray whale (*6*) and inferred by divers (*7*, *8*). The whales use oral suction to rip up patches of amphipod-rich sea floor, then expel the sediment through their baleen and consume the amphipods retained. The resulting pits on the sea floor are of sufficient size and reflectivity to be detected, measured, and mapped by side-scan sonar (Fig. 1) (*9*).

More than 4500 line-kilometers of 105-kHz side-scan sonar data were collected in the northern Bering Sea between 1977 and 1982. The records show high concentrations of feeding pits over a 22,000-km^2 area in the center of the Chirikov Basin and the southern nearshore areas of Saint Lawrence Island. Feeding pits are absent, however, in Norton Sound, the Shpanberg Strait, and immediately north of Saint Lawrence Island (Fig. 2).

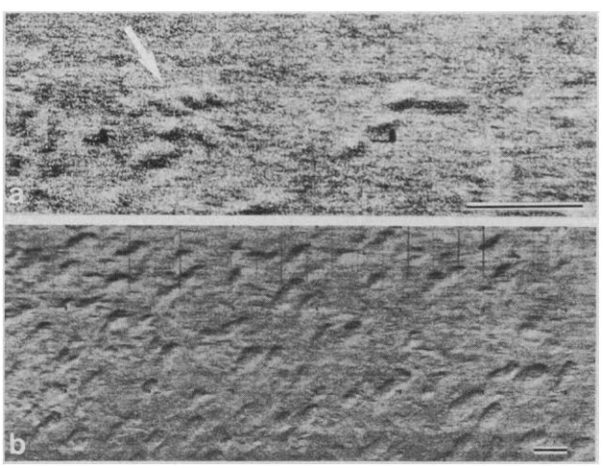

Fig. 1. Side-scan sonographs of the central Chirikov Basin floor, northeastern Bering Sea, showing (a) multiple fresh whale feeding pits and (b) older pits enlarged and oriented by the current. Scale bars, 10m.

In the northern Bering Sea the main prey of the gray whale is probably the tubicolous amphipod *Ampelisca macrocephala* (*10*), which is found in a substrate of very fine (0.125 mm), well-sorted sand (*11*). Abundant amphipod tubes commonly coalesce to form a mat that effectively fixes the sediment surface and protects it from scouring by the current (*12*). The ampeliscid amphipod distribution (*13*) closely matches the distribution of whale feeding pits and aerial sightings of feeding gray whales (Fig. 2) (*5*, *14*).

The widespread amphipod substrate was deposited at the end of the latest glacial maximum (12,000 to 10,000 years ago), when melting ice caused a marine transgression over the Bering Land Bridge. Beach sand and gravel were laid down first over the silty tundra peat of the land bridge (*15*). Then a thin (<2 m) sheet of inner-shelf fine sand was deposited. Recent input from the Yukon River has covered Norton Sound with silt and fine sand, and strong currents of the Shpanberg Strait have reworked the sediment there into coarser lag deposits. Thus only the Chirikov Basin is floored by a relict, laterally extensive sheet of homogeneous fine sand that provides the amphipod habitat (Fig. 2).

Modern processes are highly active in modifying the Bering Sea floor. The northern Bering Sea is icebound for half the year, resulting in a winter quiescence under the ice cover, except in areas where shearing ice packs cause scouring of the sea floor (*16*). Spring ice breakup (*17*) is followed by a midsummer calm. A storm season in the fall results in the triggering of gas expulsion craters (*18*), extensive scouring by currents (*19*), and high rates of sediment transport (*20*).

The whale feeding pits vary in size, shape, and density. Much of this variation can be explained as modification after formation by sediment infilling, by further feeding activity, or by current-scour enlargement. Fresh, unmodified pits seem to be oval, 0.5 to 4.0 m long, 0.5 to 2.0 m wide, and 0.1 to 0.4 m deep. They commonly occur in organized, linear, or radial groups of two to eight or more, and apparently are created by multiple feeding events (Fig. 1a) (*2*, *9*). Apparently, whales can also create pits while swimming or drifting with the current because some pits are as long as 8 m, though still of normal width.

In this seasonally dynamic region gray whales leave feeding traces that can be confused with and modified by the results of other biological and physical processes. The side-scan sonar, however, when used with a knowledge of substrate type and processes, can distinguish features created by whales from features created by other mechanisms. For example, circular gas-expulsion craters, although morphologically similar to some whale feeding pits, are restricted to muddy substrates most common in Norton Sound (*18*), where whales rarely feed (*2*).

Current scouring profoundly affects whale feeding pits. By removing the amphipod tube mat, the whales roughen the bottom and expose the underlying sediment. The pits act as loci of detritus accumulation during the summer quiescence (*21*), but during the storm season current speeds at the bottom increase to levels that can move sediment (*20*) and enlarge the pits. Commonly, erosion of the areas between individual pits of a multiple-pit system will leave a single large pit. Current-enlarged pits can be as big as 8 by 20 m and are oriented parallel to the predominant current direction (Fig. 1) (*9*).

To measure whale-induced sediment disturbance and feeding energetics, we established 16 side-scan sonar quantification stations in representative feeding areas across the Chirikov Basin (*9*). At each station we measured the length, width, orientation, and density (percentage of total area disturbed) of 64 randomly chosen whale feeding pits and compiled histograms of their length, width, and area (Fig. 3). The histogram for pit length (Fig. 3b) peaks at 2.5 m, in agreement with the histogram of gray whale gape length (Fig. 3a) but also is strongly skewed to the right, indicating enlargement by current scouring. The area histogram (Fig. 3d) shows the same skewness to the right and a slope break at 5.3 m^2. Given the marked seasonality of modifying events and using size criteria alone, we define pits smaller than 5.3 m^2 as fresh (formed during the most recent feeding season) and those larger than 5.3 m^2 as current-modified (remnants of past feeding seasons) (*22*). The density of fresh pits is low (<1 to 2 percent) near the margins of the amphipod community, as high as 12 percent in the center of the basin, and averages 5.6 percent for the entire Chirikov Basin feeding area.

Using (i) the percentage of feeding area disturbed by fresh pits (5.6 percent), (ii) the extent of gray whale feeding grounds in the northern Bering Sea (22,000 km^2), (iii) the total northern feeding range of the gray whale (1×10^6 km^2), (iv) the total number of gray whales in the eastern Pacific (16,000 in 1980) (*1*), (v) the number of days spent in the northern feeding range (180 per year), (vi) the mean concentration of amphipods (171 g/m^2) (*2, 12, 21*), and (vii) the mean daily food consumption of large cetaceans (1100 kg) (*2, 11*), we postulate that the Chirikov Basin and nearshore regions south of Saint Lawrence Island, which together represent 2 percent of the gray whale feeding range, supported a minimum of 6.5 percent of the total gray whale feeding pressure in the summer of 1980.

Geologically, gray whales profoundly disturb the substrate. Box cores of the transgressive sand sheet of the inner shelf rarely show any evidence of primary sedimentary structures (*13*), probably because of this intensive feeding activity. The whales are also responsible for triggering substantial current scouring and thus creating, in addition to their feeding pits, extensive disturbed areas favored by colonizing amphipods. The volume of sediment injected into the water column by feeding whales is at least 1.2×10^9 m^3/year, or over two times the yearly sediment load of the Yukon River. This activity, coupled with north-flowing currents, results in winnowing and northward transport of sand,

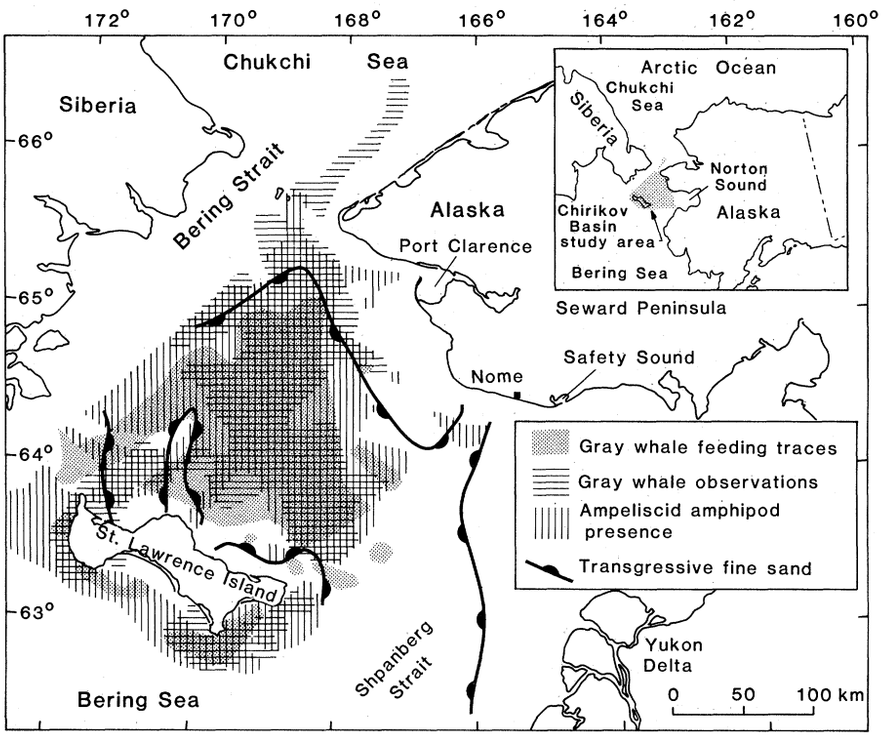

Fig. 2. Distribution of gray whale feeding pits, mapped from side-scan sonar, sightings of feeding gray whales (*9*), distribution of ampeliscid amphipods (*8*), and area of the transgressive sand sheet (the ampeliscid amphipod substrate) (*8*).

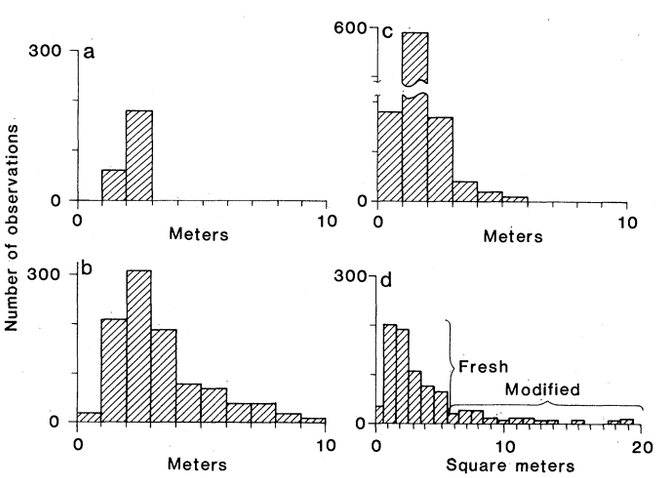

Fig. 3. (a) Histogram of gape length measure in 240 whales (*9*). (b to d) Histograms of feeding pit length (b), width (c), and area (d), based on measurements from 64 pits at each of 16 side-scan sonar stations in the Chirikov Basin.

suspension and removal of the clay and silt matrix, and recycling of nutrients that would otherwise be trapped in the sediment. Hence gray whale feeding activity may be a significant factor contributing to the high benthic productivity of the Bering Shelf.

KIRK R. JOHNSON
Department of Geology, University of Pennsylvania, Philadelphia 19104
C. HANS NELSON
Branch of Pacific Marine Geology MS999, U.S. Geological Survey, Menlo Park, California 94025

References and Notes

1. At present 16,000 gray whales exist in the eastern Pacific (S. B. Reilly, paper presented at the Fifth Biennial Conference on the Biology of Marine Mammals, Boston, 1983).
2. M. Nerini, in *The Gray Whale*: Eschrichtius robustus, M. L. Jones *et al.*, Eds. (Academic Press, New York, in press).
3. D. W. Hood and J. A. Calder, Eds., *The Eastern Bering Sea Shelf: Oceanography and Resources* (Univ. of Washington Press, Seattle, 1981), vol. 2.
4. K. J. Frost and L. F. Lowry, in *ibid.*, pp. 825–836.
5. S. Moore and D. Ljungblad, in *The Gray Whale*: Eschrichtius robustus, M. L. Jones *et al.*, Eds. (Academic Press, New York, in press).
6. G. C. Ray and W. E. Schevill, *Mar. Fish. Rev.* **36**, 31 (1974).
7. J. S. Oliver, P. N. Slattery, M. A. Silberstein, E. F. O'Connor, *Can. J. Zool.*, in press.
8. J. Hudnall, paper presented at the Fourth Biennial Conference on the Biology of Marine Mammals, 1981.
9. The side-scan sonar is a planographic sea floor surveying device that generates sonographs analogous to aerial photographs of land areas. A description of side-scan sonar methods for evaluating gray whale feeding traces is given by K. R. Johnson, C. H. Nelson, and H. L. Mitchell [*U.S. Geol. Surv. Open-File Rep. 83-727* (1983)].
10. D. W. Rice and A. A. Wolman, *Am. Soc. Mammal. Spec. Publ. No. 3* (1971).
11. S. W. Stoker, in (*3*), pp. 1066–1091.
12. C. H. Nelson, R. W. Rowland, S. Stoker, B. R. Larsen, in (*3*), pp. 1265–1296.
13. A total of 221 stations were analyzed for amphipods. Sediment data for 684 stations were from G. R. Hess, B. R. Larsen, D. Klingman, and D. Moore [*Natl. Oceanic Atmos. Adm. Outer Cont. Shelf Environ. Assess. Program Annu. Rep. RU429* (1981)].
14. L. D. Consiglieri, H. W. Braham, L. L. Jones, *Natl. Oceanic Atmos. Adm. Outer Cont. Shelf Environ. Assess. Program Q. Rep. RU-68* (1980).
15. C. H. Nelson, *Geol. Mijnbouw* **61**, 37 (1982).
16. D. R. Thor and C. H. Nelson, in (*3*), pp. 279–291.
17. W. R. Dupré, *Geol. Mijnbouw* **61**, 63 (1982).
18. C. H. Nelson, D. R. Thor, M. W. Sandstrom, K. A. Kvenvolden, *Geol. Soc. Am. Bull.* **90**, 1144 (1980).
19. M. L. Larsen, C. H. Nelson, D. R. Thor, *Environ. Geol.* **3**, 47 (1979).
20. D. A. Cacchione and D. E. Drake, *J. Geophys. Res.* **87**, 1952 (1982).
21. D. H. Thomson, unpublished manuscript.
22. M. K. Nerini and J. S. Oliver [*Oecologia (Berlin)* **59**, 224 (1983)] and Thomson (*21*), working mainly in the nearshore areas southeast of Saint Lawrence Island, did not report any evidence of enlargement of whale feeding pits by current scouring. Pit enlargement is evidently a function of local current regime as well as season. The best examples of pit enlargement by current scouring are in the east-central Chirikov Basin.
23. We thank M. Nerini, J. Oliver, and D. Thomson for discussions concerning their research. This study was funded by the Bureau of Land Management through interagency agreement with the National Oceanographic and Atmospheric Administration as part of the Outer Continental Shelf Environmental Assessment Program.

28 February 1984; accepted 31 May 1984

Magnetic Cristobalite (?): A Possible New Magnetic Phase Produced by the Thermal Decomposition of Nontronite

Abstract. *Prolonged heat treatment (>1 hour) of nontronite (an iron-rich smectite clay) at 900° to 1000°C produces a phase with some unusual magnetic properties. This new phase has a Curie temperature of 200° to 220°C, extremely high remanent coercivities in excess of 800 milliteslas, and a room-temperature coercivity dependent on the magnitude of the applied field during previous thermomagnetic cycling from above 220°C. X-ray and magnetic analyses suggest that an iron-substituted cristobalite could be responsible, in part, for these observations. Formation of this magnetic cristobalite, however, may require topotactic growth from a smectite precursor.*

In an earlier study (*1*) we reported that thermal treatment of nontronite, an iron-rich smectite clay, could cause a dramatic increase in magnetic susceptibility and saturation magnetization (σ_s). For example, when nontronite is heated at 900°C in air for only 5 minutes, an x-ray amorphous aggregate is produced with a bulk σ_s of ≈6 to 10 A-m^2/kg (products possessing these properties display what is called type 1 behavior). Nontronite is believed to be an important component of the martian regolith (*2, 3*), and this heat-treated "meta-nontronite" has composition, color, and magnetic properties consistent with those recorded by the Viking spacecraft on Mars (*1, 4*). We report here further data on the magnetic properties of thermally treated nontronite, in particular, the discovery of (i) a new, magnetic phase with a Curie temperature (T_c) of 200° to 220°C and extremely high remanent coercivity (H_r >>800 mT), produced after prolonged heating at 900°C (behavior hereafter referred to as type 2), and (ii) the identification of the type 1 phase as a maghemite thermally stable to at least 1000°C. The formation of these two magnetic phases prompts considerations concerning the thermal transformations of iron-rich clay minerals, the stability and metastability of maghemite, and the possible applications of these phases as high-coercivity permanent magnet and magnetic tape materials.

A representative series of magnetization versus temperature (σ-T) curves are shown in Fig. 1 for samples of Manito nontronite (*5*) annealed at 900°C for periods ranging from 5 minutes to 193 hours. Two types of σ-T behavior are apparent in Fig. 1. As was also true for all other nontronite samples studied, after annealing times less than approximately 3 hours the σ-T curves are reversible (σ_f/σ_i ≈1, where σ_f is the final magnetization after heating and σ_i is the initial magnetization before heating) and the magnetization decreases almost linearly with temperature (Fig. 1a). This σ-T behavior is another characteristic of the type 1 phase. Magnetic properties for samples exhibiting type 1 behavior also include (i) σ_s ≈6 to 10 A-m^2/kg, (ii) superparamagnetic behavior with an effective magnetic grain size of 70 to 150 Å, and (iii) no distinct Curie temperature (*1, 6*).

After samples have been heated for longer than 5 hours, the σ-T behavior begins to transform from type 1 to type 2, which becomes increasingly prominent after 13 hours. Type 2 behavior is characterized by (i) an increase in magnetization with temperature to ≈150°C (T_{max}), (ii) an apparent T_c of 200°C to 220°C, and (iii) a large increase in magnetization after heating (σ_f/σ_i ≈2 to 5) (Fig. 1, c to f). As the annealing time increases beyond 13 hours, both T_{max} and σ_f/σ_i increase.

In addition to the irreversible σ-T behavior, type 2 samples are also unusual with respect to thermomagnetic cycling in an applied field. Initial σ-T curves exhibit the typical type 2 behavior (type 2a, Fig. 2a), but, if the applied field during cooling from above 220°C is >4 mT, then during subsequent thermomagnetic cycling the σ-T curves become almost reversible (σ_f/σ_i ≈1 to 1.5) and the increase in magnetization during heating disappears (type 2b, Fig. 2b). If, however, the applied field during cooling from above 220°C is <4 mT, then the typical type 2a behavior returns during the next thermomagnetic cycle. The change from type 2a to type 2b is reversible, the behavior being determined by the magnitude of the applied field during cooling from above 200°C. The applied field also determines the values of T_{max} and σ_f/σ_i; an increase in the field causes both quantities to decrease.

Other magnetic properties for samples exhibiting type 2 behavior include the following: (i) a bulk σ_s of ≈3 to 5 A-m^2/kg; (ii) extremely high H_r, in excess of 800 mT; and (iii) high values of the ratio